



Continuous changes in electrical conductivity of sodium aluminate solution in seeded precipitation



Gui-hua LIU, Zheng LI, Tian-gui QI, Qiu-sheng ZHOU, Zhi-hong PENG, Xiao-bin LI

School of Metallurgy and Environment, Central South University, Changsha 410083, China

Received 18 January 2015; accepted 29 July 2015

Abstract: The mechanism of seeded precipitation of sodium aluminate solution was studied by measuring the seeded-precipitation rate and electrical conductivity online, as well as calculating the activity and fraction of ion pair. The results show that the electrical conductivity of sodium aluminate slurry linearly decreases with increasing aluminum hydroxide addition. Moreover, both the electrical conductivity of slurry and the difference in electrical conductivity between sodium aluminate solution and slurry remarkably decline in the first 60 min before gradually increasing in the preliminary 10 h and finally reaching almost the same level after 10 h. In low Na_2O concentration solution the activities of NaOH and $\text{NaAl}(\text{OH})_4$ in seeded precipitation are high, which can enlarge the difference in conductivity between slurry and solution. Additionally, more ion pairs exist in solution in preliminary seeded precipitation, and the adsorption of $\text{Na}^+\text{Al}(\text{OH})_4^-$ on seed surface is likely to break the equilibrium of ion pair formation and to decrease the difference in conductivity in preliminary seeded precipitation.

Key words: sodium aluminate solution; seeded precipitation; electrical conductivity; activity coefficient; ion pair

1 Introduction

Seeded precipitation for preparing aluminum hydroxide (AH) is used in alumina refineries, including AH precipitated from pregnant sodium aluminate solution ($\text{Al}(\text{OH})_4^- \rightleftharpoons \text{Al}(\text{OH})_3 + \text{OH}^-$) and coarse AH crystallized by nucleation [1], agglomeration, and growth [2]. The mechanism of seeded precipitation was extensively studied by solubility of AH [3–5], electrical conductivity [6], surface tension [7], viscosity [8], activity [9] in the solution and the structure of aluminate ion. Based on kinetic studies [10], various methods, such as varying the concentration of caustic soda or alumina [11], adding active seed [12] and crystallization additives [13], irradiating with ultrasonic sound [14], and setting up an additional electric field or magnetic field [15] have been used to increase precipitation rate. However, the seeded-precipitation ratio in theory is greater than that in practice in the precipitation time range of 30–55 h. Low seeded-precipitation rate, long precipitation time, and low output of equipment are the disadvantages in alumina refineries for preparing sandy alumina. The main reason lies in the uncertainty of the

mechanism in seeded precipitation with high seed content.

The structure of aluminate ion is the key to understand the mechanism of seeded precipitation. Numerous researchers have studied the structure of aluminate ion in synthetic solution or solution from alumina refinery by filtration or centrifugation [16]. By measuring electrical conductivity, surface tension, viscosity or obtaining ultraviolet spectrum, infrared spectrum, Raman spectrum, or nuclear magnetic resonance (NMR) [17–19], the following conclusions about the aluminate ion structure can be drawn. Firstly, aluminate ion structure varies with the concentration, preparation method and hold time of solution [20–22]. Secondly, tetrahedral $\text{Al}(\text{OH})_4^-$ is the dominant form in sodium aluminate solution, though dimer ion $[\text{Al}_2\text{O}(\text{OH})_6]^{2-}$ and other aluminate ion may exist in concentrated solution [6]. Thirdly, polymer aluminate anion, acting as growth units in precipitation, is aggregated from $\text{Al}(\text{OH})_4^-$ in seeded precipitation [23]. Fourthly, Na^+ , OH^- or H_2O also affect the forms of the aluminate ion because of the formation of ion hydration or ion pair [24,25]. All results suggest that various conversions among aluminate ions extremely affect the

seeded precipitation. However, we often neglect the significant difference in aluminate ion structure in solution and slurry with high content of seed, and pay little attention on the influence of seed on the aluminate structure. Moreover, the changes in structure and mechanism of the preliminary period in seeded precipitation are rarely studied.

In this work, we investigated the influence of AH seed and solution composition on the electrical conductivity of sodium aluminate solution by detecting electrical conductivity online, discussed the variation of electrical conductivity based on the calculation of mean activity coefficient and ion pair, and further explored the mechanism of seeded precipitation. All results will benefit the development of new technology for seeded precipitation.

2 Experimental

2.1 Materials

Sodium aluminate solution was prepared with analytically pure AH and sodium hydroxide (Xilong Chemical Co., Ltd.). AH was added as the seed in precipitation. Seeded precipitation was conducted in an 1.5 L steel-tank which was heated by water bath. The electrical conductivity of solution was measured online by M300 conductivity meter (METTLER TOLEDO, Shanghai, Co., Ltd.).

2.2 Experimental procedures

1 L sodium aluminate solution with $\alpha_k=1.41$ (molar ratio of caustic soda (Na_2O) to alumina (Al_2O_3) in sodium aluminate solution) was added into 1.5 L tank, heated to 55 °C and stirred at 150 r/min. AH was then added according to the seed coefficient $K_f=3.4$ (mass ratio of alumina in seed to alumina in solution). Meanwhile, the online conductivity meter was turned on, and the data were recorded simultaneously. Lastly, the slurry in seeded precipitation was obtained at a given time, and Na_2O and Al_2O_3 concentrations were detected following the separation of solid and solution.

2.3 Methods

Na_2O and Al_2O_3 concentrations in sodium aluminate solution were determined by titration. Afterwards, the seeded-precipitation rate (η) was calculated according to the following equation:

$$\eta = \frac{\alpha_{kt} - \alpha_{k0}}{\alpha_{kt}} \times 100\% \quad (1)$$

where subscripts 0 and t stand for initial time and time t in seeded precipitation, respectively.

The difference in conductivity value ($\Delta\sigma$) in seeded precipitation was obtained by subtracting the electrical

conductivity of the slurry from the electrical conductivity of the solution.

3 Results and discussion

3.1 Electrical conductivity of slurry in seeded precipitation at constant temperature

3.1.1 Influence of AH addition on electrical conductivity of slurry

The strong polarity of AH highly affects the electrical conductivity of sodium aluminate solution, as shown in Fig. 1.

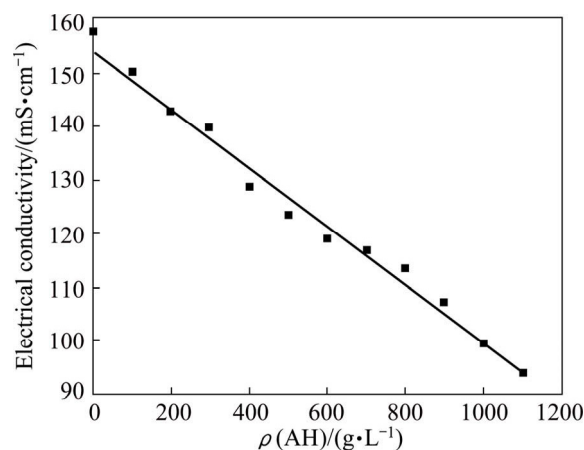


Fig. 1 Influence of AH addition on electrical conductivity of slurry

The test conditions are as follows: $\rho(\text{Na}_2\text{O})=130 \text{ g/L}$; $\alpha_k=1.45$; seeded precipitation temperature 55 °C; stirring speed 150 r/min.

The electrical conductivity (σ) of the slurry linearly decreases with increasing AH concentration in the solution of 130 g/L Na_2O (Fig. 1). The decrease of the electrical conductivity of the slurry can be attributed to the inversely induced-electrical field, resulting from the polar surface of AH. Afterwards, linear equation is obtained:

$$\sigma = -0.054\rho(\text{AH}) + 153.72 \quad (2)$$

where σ is the electrical conductivity, and $\rho(\text{AH})$ is the AH concentration, g/L. The correlation coefficient R^2 is 0.985.

Based on Eq. (2), the influence of AH (seed and AH precipitated from solution) on the electrical conductivity of the slurry can be discussed.

3.1.2 Changes in electrical conductivity in preliminary seeded precipitation

The stability of the sodium aluminate solution is broken after adding seed. However, few researchers have reported changes in electrical conductivity in preliminary seeded precipitation. The electrical conductivity of sodium aluminate solution after adding seed in the first

60 s is shown in Fig. 2.

Interestingly, the electrical conductivity of the slurry sharply decreases at the first 30 s and then slowly increases, a minimum value at 37 s can be observed in Fig. 2. However, the seeded-precipitation rate is almost close to zero within 60 s because of good metastability of the sodium aluminate solution. This fact implies that aluminate ion structure remarkably changes in preliminary seeded precipitation.

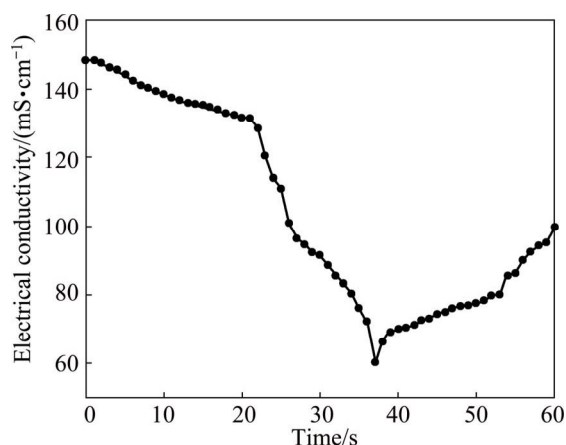


Fig. 2 Effect of time on electrical conductivity of slurry in preliminary precipitation ($\rho(\text{Na}_2\text{O})=130 \text{ g/L}$, $\alpha_k=1.45$, constant temperature 55°C , $K_r=3.4$, stirring speed 150 r/min)

3.1.3 Influence of caustic soda concentration on seeded-precipitation rate and electrical conductivity of slurry

The effect of Na_2O concentration and time on the seeded-precipitation rate at 55°C is presented in Fig. 3.

As shown in Fig. 3, the seeded-precipitation rate gradually increases with prolonging seeded precipitation time, and the seeded-precipitation rate in $130 \text{ g/L Na}_2\text{O}$ solution is greater than that in $200 \text{ g/L Na}_2\text{O}$ solution. However, the seeded-precipitation rate is only 0.62% in

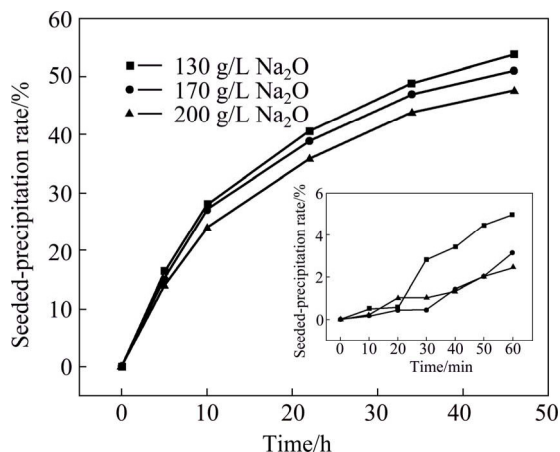


Fig. 3 Effect of Na_2O concentration on seeded-precipitation rate in sodium aluminate solution ($\alpha_k=1.45$, 55°C , 150 r/min , $K_r=3.4$)

the $130 \text{ g/L Na}_2\text{O}$ solution at 20 min. Afterwards, significant increases with seeded-precipitation rate of 2.78% and 5.01% can be observed at 30 and 60 min, respectively. By contrast, the seeded-precipitation rates is less than 1% in sodium aluminate solutions of 170 and $200 \text{ g/L Na}_2\text{O}$ at 20 min, and low seeded-precipitation rates of 2% and 3% can be observed at 60 min for 170 and $200 \text{ g/L Na}_2\text{O}$ solution, respectively. Hence, few AH is precipitated in the first 1 h in the concentrated solution.

The electrical conductivity of the slurry in seeded precipitation is shown in Fig. 4.

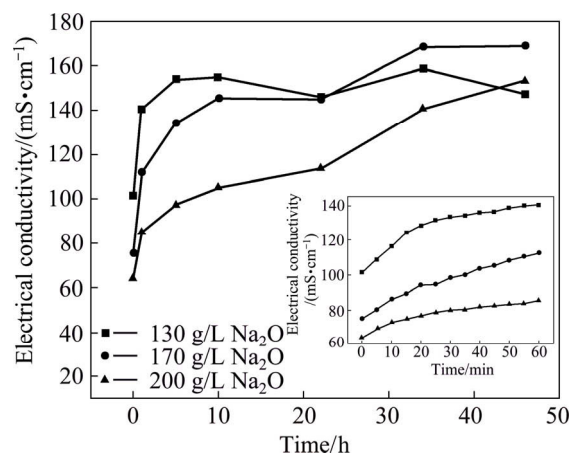


Fig. 4 Effect of time on electrical conductivity of slurry in seeded precipitation ($\alpha_k=1.45$, 55°C , 150 r/min , $K_r=3.4$)

Figure 4 indicates that the electrical conductivity of the slurry sharply increases at the first 5 h, and then almost levels off or increases very slowly in solution of $200 \text{ g/L Na}_2\text{O}$, differing from the variation of seeded-precipitation rates in Fig. 3. Meanwhile, the conductivity in the dilute solution is greater than that in the concentrated solution, though more ions may exist in the concentrated solution. In addition, during the preliminary 60 min, electrical conductivity of the $130 \text{ g/L Na}_2\text{O}$ solution more remarkably increases than that of the 170 and $200 \text{ g/L Na}_2\text{O}$ solutions, which is in accordance with the seeded-precipitation rate in different solutions. The reason is mainly attributed to releasing free OH^- ion in seeded precipitation according to the following equation:



Generally, Na^+ concentration is constant in seeded precipitation at a given Na_2O concentration, and the migration rate of OH^- is faster than that of $\text{Al}(\text{OH})_4^-$ and $\text{Al}_2\text{O}(\text{OH})_6^{2-}$. Thus, the electrical conductivity of the solution synchronously increases with the increase of the seeded-precipitation rate in theory. However, the electrical conductivity of the slurry sharply increases at the first 5 h, though all seeded-precipitation rates are less

than 15%, and then slowly increase (almost levels off) after 10 h, though the seeded-precipitation rate still noticeably increases. All the above facts imply that the electrical conductivity is related to the variation of aluminate ions structure besides OH^- .

3.2 Influence of AH addition on electrical conductivity of sodium aluminate solution

The results in Fig. 1 show a linear relationship between the electrical conductivity of slurry and AH concentration, but the effect of the seed on the electrical conductivity of the solution in seeded precipitation remains unknown. Therefore, the difference in electrical conductivity ($\Delta\sigma$) between slurry and solution is obtained according to the following procedures: obtaining the electrical conductivity of sodium aluminate solution at different concentrations, and subtracting the electrical conductivity from the electrical conductivity of the solution.

Electrical conductivity of sodium aluminate solution was measured according to an orthogonal design method at α_k of 1.45–3.30, $\rho(\text{Na}_2\text{O})$ of 123.03–205.60 g/L and 55 °C. The data are listed in Table 1.

Table 1 Electrical conductivities of sodium aluminate solution at 55 °C and different Na_2O concentrations

α_k	$\rho(\text{Na}_2\text{O})/(\text{g}\cdot\text{L}^{-1})$	$\sigma/(\text{mS}\cdot\text{cm}^{-1})$
1.45	123.03	163.89
1.45	161.67	139.00
1.45	183.02	114.92
1.45	205.39	111.96
2.00	126.08	270.28
2.00	164.11	207.21
2.00	213.40	197.70
3.30	128.12	312.58
3.30	170.00	315.66
3.30	205.60	309.15

The following equation was obtained by data fitting:

$$\sigma = 176.96 - 3.67\rho(\text{Na}_2\text{O}) + 249.21\alpha_k + 0.0096\rho^2(\text{Na}_2\text{O}) - 31.39\alpha_k^2 \quad (4)$$

The correlation coefficient R^2 is 0.99.

Thus, the electrical conductivity of sodium aluminate solution in seeded precipitation was calculated according to Eq. (4) based on Na_2O and Al_2O_3 concentrations in seeded precipitation. The difference in electrical conductivity ($\Delta\sigma$) in seeded precipitation is shown in Fig. 5.

Figure 5 shows that $\Delta\sigma$ remarkably decreases before 2.5 h and then sharply increases, differing from the results in Fig. 4. Moreover, $\Delta\sigma$ of 130 g/L Na_2O solution

increases more significantly after 25 h compared with that of the 170 and 200 g/L Na_2O solutions. The increase in electrical conductivity of the solution is more than that of the slurry in seeded precipitation due to more OH^- forming. Additionally, the sharp decrease of the electrical conductivity before 2.5 h is also attributed to notable changes in aluminate ion structure, confirming the significant influence of AH seed on the aluminate ion structure in Fig. 2. Both imply that aluminate ion complicatedly varies in seeded precipitation, which subsequently influences the mechanism of seeded precipitation.

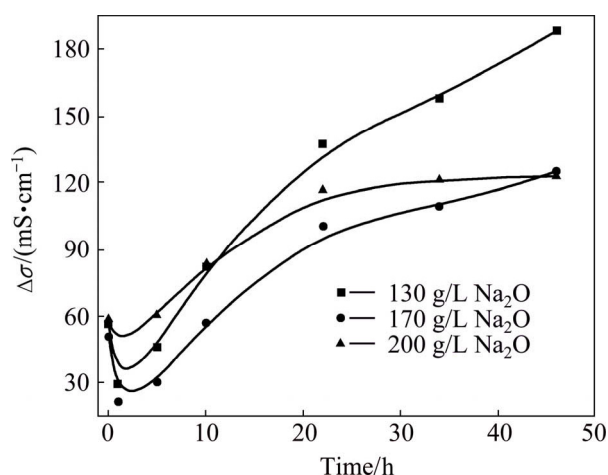


Fig. 5 Effect of time on electric conductivity difference in seeded precipitation ($\alpha_k=1.45$, 55 °C, 150 r/min, $K_f=3.4$)

3.3 Activity and fraction of ion pair for sodium aluminate in seeded precipitation

3.3.1 Activity of sodium aluminate and sodium hydroxide

Based on mean activity coefficient calculation model of sodium aluminate in $\text{NaOH}-\text{NaAl}(\text{OH})_4-\text{H}_2\text{O}$ system derived from Pitzer equation [3], changes in the mean activity coefficient of NaOH and $\text{NaAl}(\text{OH})_4$ in seeded precipitation can be determined. The activities of NaOH and $\text{NaAl}(\text{OH})_4$ are obtained according to Eq. (5).

$$a_i = (a_{\pm})^2 = (m_{\pm}\gamma_{\pm})^2 = m\gamma_{\pm}^2 \quad (5)$$

where subscript i stands for i substance, m and γ_{\pm} represent mass molar concentration (mol/kg) and the mean activity coefficient, respectively. The results are presented in Fig. 6.

The results in Figs. 6(a) and (b) show that the mean activity coefficient of NaOH gradually decreases, whereas its activity slowly increases because of NaOH formation in seeded precipitation according to Eq. (3). Meanwhile, low concentration of Na_2O increases the activity of NaOH compared with the electrical conductivity in 170 and 200 g/L Na_2O solutions, which leads to the increase of the electrical conductivity and

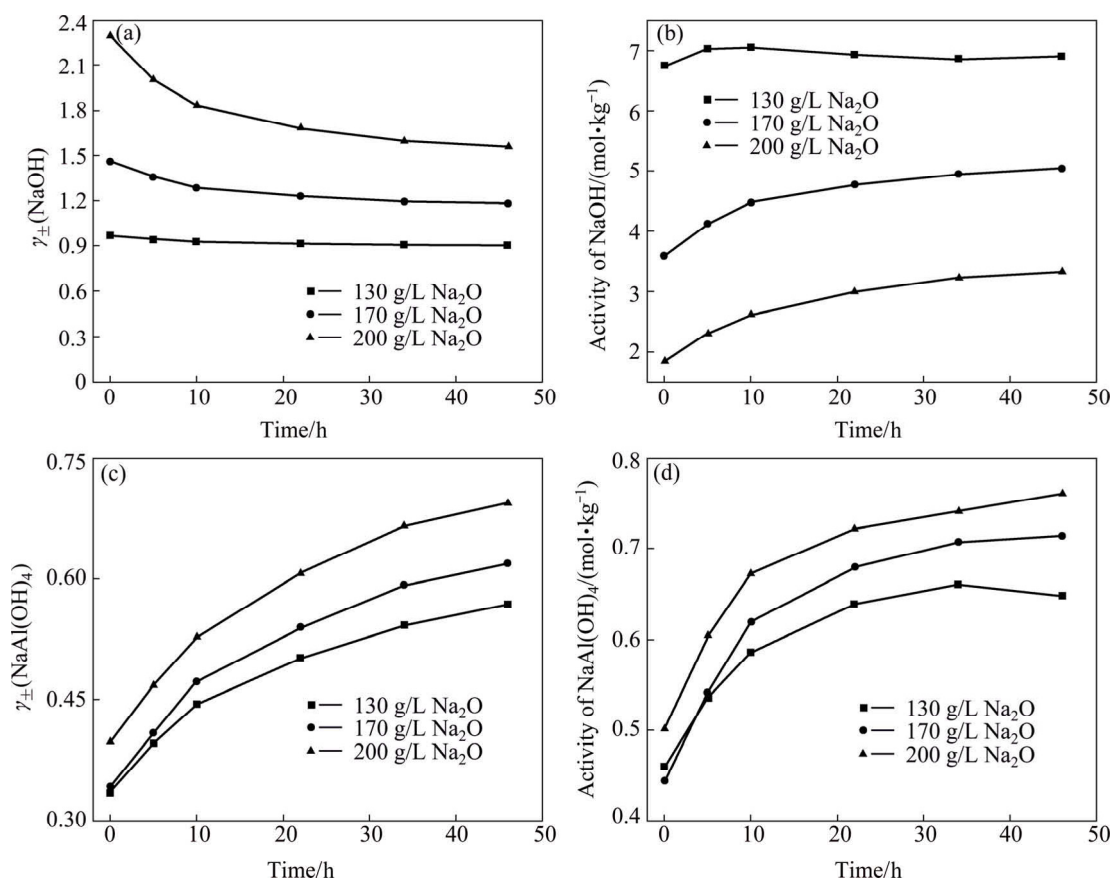


Fig. 6 Changes in mean activity coefficients and activities of sodium hydroxide and sodium aluminate in seeded precipitation

seeded precipitation. By contrast, the mean activity coefficient and activity of sodium aluminate increase in seeded precipitation, but its activity is lower than that of NaOH in seeded precipitation. Thus, the small increase of NaOH activity mainly is ascribed to the slow increase of electrical conductivity in Figs. 4 and 5.

However, the remarkable decrease of $\Delta\sigma$ in preliminary seeded precipitation may be caused by the formation of ion pair.

3.3.2 Changes in fraction of ion pair in seeded precipitation

Ion pair can be easily found in the concentrated solution. Given that various ion pairs may be formed in the sodium aluminate solution [26] and ion pair simplification is adopted, two kinds of ion pairs Na^+OH^- [3] and $\text{Na}^+\text{Al}(\text{OH})_4^-$ [27] are calculated according to Bjerrum theory. The equation is written as follows:

$$\theta = \frac{4\pi Nc}{1000} \left(\frac{|Z_i Z_j| e^2}{\epsilon kT} \right)^3 Q(b) \quad (6)$$

$$b = \frac{|Z_i Z_j| e^2}{\epsilon kTa} \quad (7)$$

where θ is the ion associated degree, N is the number of ions, c is the molar concentration, Z_i and Z_j are ionic

charges of ions i and j , respectively, $Z_i Z_j$ is associated with ionic charge number, e is the electric charge, ϵ is the dielectric constant of solution, and k is the Boltzmann constant, T is the thermodynamic temperature, a is the distance of ion pair.

The distances between Na^+ and OH^- , Na^+ and $\text{Al}(\text{OH})_4^-$ are 3.31 and 3.595 Å, respectively. Temperature is 328.15 K. Meanwhile, the total concentration of caustic soda (NaOH_T) is equal to the sum of the concentration of sodium hydroxide $c(\text{NaOH}_f)$ and sodium aluminate, as shown in Eq. (8):

$$m(\text{NaOH}_T) = m(\text{NaOH}_f) + m(\text{NaAl}(\text{OH})_4) \quad (8)$$

The fraction of ion pair is shown in Table 2.

Table 2 shows that the ion pair of Na^+OH^- is easily formed. Moreover, increasing the alumina concentration

Table 2 Fraction of ion pair for Na^+OH^- and $\text{Na}^+\text{Al}(\text{OH})_4^-$ in different solutions

α_k	Fraction of ion pair	
	Na^+OH^- at $m(\text{NaOH}_T)$	$\text{Na}^+\text{Al}(\text{OH})_4^-$ at $m(\text{NaOH}_T)$
	of 2 mol/kg	of 3 mol/kg
1.5	0.79	0.22
3.0	0.20	0.11
5.0	0.099	0.065

favors the formations of Na^+OH^- and $\text{Na}^+\text{Al}(\text{OH})_4^-$. The ion pairs of Na^+OH^- and $\text{Na}^+\text{Al}(\text{OH})_4^-$ still occur in the later seeded precipitation because the fractions of ion pairs of Na^+OH^- and $\text{Na}^+\text{Al}(\text{OH})_4^-$ in solution of $\alpha_k=3.0$ are 0.20 and 0.11, respectively. These results verify that ion pairs of Na^+OH^- and $\text{Na}^+\text{Al}(\text{OH})_4^-$ in seeded precipitation affect the activity of aluminate ion and contribute to changes in $\Delta\sigma$.

Ion pair of $\text{Na}^+\text{Al}(\text{OH})_4^-$ exists in sodium aluminate solution, resulting in the low electrical conductivity as shown in Fig. 4. Meanwhile, AH surface is characterized by negative charge precipitated from sodium aluminate solution [27]. When AH seed is added, the adsorption of $\text{Na}^+\text{Al}(\text{OH})_4^-$ on seeded surface also breaks up the following equilibrium: $\text{Na}^+ + \text{Al}(\text{OH})_4^- \rightleftharpoons \text{Na}^+\text{Al}(\text{OH})_4^-$.

Consequently, more free Na^+ and $\text{Al}(\text{OH})_4^-$ in solution form $\text{Na}^+\text{Al}(\text{OH})_4^-$ and subsequently decrease the electrical conductivity of the solution. Thus, significant decrease in $\Delta\sigma$ in the preliminary period of seeded precipitation as mentioned in Fig. 6 can be observed. The finding provides a valuable reference in raising seeded precipitation rate. However, more evidences are required to support this conclusion.

4 Conclusions

1) The electrical conductivity of slurry linearly decreases with AH addition increasing in sodium aluminate solution; it sharply decreases at the preliminary stage and then remarkably increases, and almost levels off after 10 h in seeded precipitation.

2) The activities of NaOH and $\text{NaAl}(\text{OH})_4$ increase in seeded precipitation, and the high activity in dilute solution benefits the electrical conductivity. High concentration and low molar ratio facilitate the formation of ion pair, and ion pair still occurs in later seeded precipitation.

3) The activity of NaOH mainly contributes to the increase in electrical conductivity and difference electrical conductivity change in the seeded precipitation. The adsorption of $\text{Na}^+\text{Al}(\text{OH})_4^-$ on seed surface may lead to the sharp decrease in electrical conductivity in preliminary seeded precipitation.

References

- [1] SEYSSIECQ I, VEESLER S, BOISTELLE R, LAMÉ RANT J M. Agglomeration of gibbsite $\text{Al}(\text{OH})_3$ crystals in Bayer liquors: Influence of the process parameters [J]. Chemical Engineering Science, 1998, 53(12): 2177–2185.
- [2] ZHOU Qiu-sheng, PENG Dian-jun, PENG Zhi-hong, LIU Gui-hua, LI Xiao-bin. Agglomeration of gibbsite particles from carbonation process of sodium aluminate solution [J]. Hydrometallurgy, 2009, 99(3–4): 163–169.
- [3] LI Xiao-bin, YAN Li, ZHOU Qiu-sheng, LIU Gui-hua, PENG Zhi-hong. Thermodynamic model for equilibrium solubility of gibbsite in concentrated NaOH solutions [J]. Transactions of Nonferrous Metals Society of China, 2012, 22(2): 447–455.
- [4] LI Xiao-bin, YAN Li, ZHAO Dong-feng, ZHOU Qiu-sheng, LIU Gui-hua, PENG Zhi-hong, YANG Shuai-shuai, QI Tian-gui. Relationship between $\text{Al}(\text{OH})_3$ solubility and particle size in synthetic Bayer liquors [J]. Transactions of Nonferrous Metals Society of China, 2013, 23(5): 1472–1479.
- [5] BROWNE G R, FINN C W P. The effects of aluminum content, temperature and impurities on the electrical conductivity of synthetic bayer liquors [J]. Metallurgical Transactions B, 1981, 12(3): 487–492.
- [6] WANG Ya-jing, ZHAI Yu-chun, TIAN Yan-wen, JI Zhi-ling, QU Xing-tao, YANG Xing-man. Mathematical model on surface tension of aluminate solution [J]. Nonferrous Metals, 2004, 56(3): 60–62. (in Chinese)
- [7] LI J, PRESTIDGE C A, ADDAI-MENSAH J. Viscosity, density, and refractive index of aqueous sodium and potassium aluminate solutions [J]. Journal of Chemical and Engineering Data, 2000, 45(4): 665–671.
- [8] WESOŁOWSKI D J. Aluminum speciation and equilibria in aqueous solution: I. The solubility of gibbsite in the system $\text{Na-K-Cl-OH-Al}(\text{OH})_4$ from 0 to 100 °C [J]. Geochimica et Cosmochimica Acta, 1992, 56(3): 1065–1091.
- [9] LI Xiao-bin, ZHAO Dong-feng, YANG Shuai-shuai, WANG Dan-qin, ZHOU Qiu-sheng, LIU Gui-hua. Influence of thermal history on conversion of aluminate species in sodium aluminate solution [J]. Transactions of Nonferrous Metals Society of China, 2014, 24(10): 3348–3355.
- [10] FARHADI F, BABAHEIDARY M B. Mechanism and estimation of $\text{Al}(\text{OH})_3$ crystal growth [J]. Journal of Crystal Growth, 2002, 234(4): 721–730.
- [11] LIU Gui-hua, WANG Peng, QI Tian-gui, LI Xiao-bin, TIAN Lü, ZHOU Qiu-sheng, PENG Zhi-hong. Variation of soda content in fine alumina trihydrate by seeded precipitation [J]. Transactions of Nonferrous Metals Society of China, 2014, 24(1): 243–249.
- [12] ZENG Ji-shu, YIN Zhou-lan, CHEN Qi-yuan. Intensification of precipitation of gibbsite from seeded caustic sodium aluminate liquor by seed activation and addition of crown ether [J]. Hydrometallurgy, 2007, 89(1–2): 107–116.
- [13] WU Yu-sheng, YU Hai-yan, YANG Yi-hong, BI Shi-wen. Effects of additives on agglomeration and secondary nucleation in seed precipitation in sodium aluminate solution [J]. Journal of Chemical Industry and Engineering, 2005, 56(12): 2434–2439. (in Chinese)
- [14] ZHANG Bin, LI Jie, CHEN Qi-yuan, CHEN Guo-hui. Precipitation of $\text{Al}(\text{OH})_3$ crystals from supersaturated sodium aluminate solution irradiated with ultrasonic sound [J]. Minerals Engineering, 2009, 22(9–10): 853–858.
- [15] LI Xiao-bin, WANG Dan-qin, ZHOU Qiu-sheng, LIU Gui-hua, PENG Zhi-hong. Influence of magnetic field on the seeded precipitation of gibbsite from sodium aluminate solution [J]. Minerals Engineering, 2012, 32: 12–18.
- [16] GALE J D, ROHL A L, WATLING H R, PARKINSON G M. Theoretical investigation of the nature of aluminum-containing species present in alkaline solution [J]. Journal of Physical Chemistry B, 1998, 102(50): 10372–10382.
- [17] CARREIRA L A, MARONI V A, SWAINE J W Jr, PLUMB R C. Raman and infrared spectra and structures of the aluminate ions [J]. The Journal of Chemical Physics, 1966, 45(6): 2216–2220.
- [18] LI H X, ADDAI-MENSAH J, THOMAS J C, GERSON A. The influence of Al (III) supersaturation and NaOH concentration on the rate of crystallization of $\text{Al}(\text{OH})_3$ precursor particles from sodium aluminate solutions [J]. Journal of Colloid and Interface Science, 2005, 286(2): 511–519.

- [19] SIPOS P, HEFTER G, MAY P M. ^{27}Al NMR and Raman spectroscopic studies of alkaline aluminate solutions with extremely high caustic content—Does the octahedral species $\text{Al}(\text{OH})_6^{3-}$ exist in solution? [J]. *Talanta*, 2006, 70(4): 761–765.
- [20] BRADLEY S M, HANNA J V. ^{27}Al and ^{23}Na MAS NMR and powder X-ray diffraction studies of sodium aluminate speciation and the mechanistics of aluminum hydroxide precipitation upon acid hydrolysis [J]. *Journal of the American Chemical Society*, 1994, 116(17): 7771–7783.
- [21] RADNAI T, MAY P M, HEFTER G T, SIPOS P. Structure of aqueous sodium aluminate solutions: A solution X-ray diffraction study [J]. *The Journal of Physical Chemistry A*, 1998, 102(40): 7841–7850.
- [22] SWEEGERS C, MEEKES H, ENCKEVORT V W J P. Growth rate analysis of gibbsite single crystals growing from aqueous sodium aluminate solutions [J]. *Crystal Growth & Design*, 2004, 4(1): 185–198.
- [23] GUTOWSKY H S, SAIKA A. Dissociation, chemical exchange, and the proton magnetic resonance in some aqueous electrolytes [J]. *The Journal of Chemical Physics*, 1953, 21(10): 1688–1694.
- [24] LIPPINCOTT E R, PSELLOS J A, TOBIN M C. The Raman spectra and structures of aluminate and zincate ions [J]. *The Journal of Chemical Physics*, 1952, 20(3): 536.
- [25] MOOLENAAR R J, EVANS J C, MCKEEVER L D. Structure of the aluminate ion in solutions at high pH [J]. *The Journal of Physical Chemistry*, 1970, 74(20): 3629–3636.
- [26] SIPOS P. The structure of $\text{Al}(\text{III})$ in strong alkaline aluminate solutions—A review [J]. *Journal of Molecular Liquids*, 2009, 146(1–2): 1–14.
- [27] LI Yun-feng. Study on surface modification and flame retardant of super-fine aluminium trihydroxide powder [D]. Changsha: Central South University, 2012. (in Chinese)

铝酸钠溶液种分过程中电导率的连续变化规律

刘桂华, 李 铮, 齐天贵, 周秋生, 彭志宏, 李小斌

中南大学 冶金与环境学院, 长沙 410083

摘 要: 通过在线测定种分过程铝酸钠溶液的电导率, 计算种分过程中组分的活度和缔合度, 研究铝酸钠溶液的种分机理。结果表明: 浆液电导率随着氢氧化铝含量增加呈线性降低; 种分初期 60 min 内浆液电导率和铝酸钠溶液和浆液电导率的差值均显著降低, 然后随种分的进行而显著升高, 但在 10 h 后电导率增大幅度变小。低浓度溶液中 NaOH 和 $\text{NaAl}(\text{OH})_4$ 活度较高, 有利于种分, 使溶液和浆液间电导率差值增大; 且种分初期溶液中离子对多, 有利于 $\text{Na}^+\text{Al}(\text{OH})_4^-$ 吸附在晶种表面, 导致溶液中生成离子对的平衡被打破, 从而使电导率差值减小。

关键词: 铝酸钠溶液; 种分; 电导率; 活度因子; 离子对

(Edited by Wei-ping CHEN)